

# $^1\text{H}$ , $^2\text{H}$ and $^{13}\text{C}$ NMR Studies of Cation Dynamics in a Layered Perovskite-Type Incommensurate Compound $(n\text{-C}_3\text{H}_7\text{NH}_3)_2\text{CdCl}_4$

Koh-ichi Suzuki, Hiroki Fujimori, Tetsuo Asaji, Shin'ichi Ishimaru<sup>a</sup>, and Ryuichi Ikeda<sup>a</sup>

Department of Chemistry, College of Humanities and Sciences, Nihon University, Sakurajosui, Setagaya-ku, Tokyo 156-8550, Japan

<sup>a</sup> Department of Chemistry, University of Tsukuba, Tsukuba 305-8571, Japan

Reprint requests to Dr. K. S.; Fax: +81-3-5317-9433, E-mail: suzuki\_k@chs.nihon-u.ac.jp

Z. Naturforsch. **57 a**, 451–455 (2002); received December 17, 2001

Presented at the XVth International Symposium on Nuclear Quadrupole Interactions, Hiroshima, Japan, September 9-14, 2001.

Cation dynamics in  $(n\text{-C}_3\text{H}_7\text{NH}_3)_2\text{CdCl}_4$  and  $(n\text{-C}_3\text{H}_7\text{ND}_3)_2\text{CdCl}_4$  were investigated by  $^1\text{H}$ ,  $^2\text{H}$ , and  $^{13}\text{C}$  NMR measurements. An overall motion of the cation being associated with the fluctuation of the molecular axis is suggested to be activated with increasing temperature. The cationic motion is enhanced at the counter side of the  $-\text{NH}_3^+$  group probably because the group is bound with the inorganic layer through the N-H...Cl hydrogen bonds.

**Key words:**  $^1\text{H}$  NMR  $T_1$ ;  $^2\text{H}$  NMR Spectra;  $^{13}\text{C}$  MAS NMR  $T_1$ ; Cation Dynamics; Phase Transition.

## 1. Introduction

Layered perovskite-type compounds with the general formula  $(\text{C}_n\text{H}_{2n+1}\text{NH}_3)_2\text{MX}_4$ , where M and X express divalent metals and halogen ions, respectively, have interesting electronic properties as nonlinear optical materials [1 - 3], and the dynamics of their cations in the two-dimensional structure are useful as model of lipid membranes [4, 5]. These compounds consist of inorganic layers of corner-sharing  $\text{MX}_6$  octahedra and organic layers of alkylammonium ions. The  $-\text{NH}_3^+$  polar heads of the alkylammonium, forming  $\text{NH}\dots\text{X}$  hydrogen bonds with halogen atoms, occupy cavities among the octahedra. Some of propylammonium salts with this structure have been reported to undergo a transition to the incommensurate (IC) phase [6 - 9]. The cation dynamics and interionic interactions through hydrogen bonds are expected to be closely related with the physical properties and mechanisms of structural phase transitions in these materials.

Bis(*n*-propylammonium) tetrachlorocadmate ( $n\text{-C}_3\text{H}_7\text{NH}_3)_2\text{CdCl}_4$  (abbreviated to PACC), belonging to this group of layered compounds have been reported to undergo phase transitions at 178.7, 156.8

and 105.5 K [10] and show a normal (N) - IC - commensurate (C) - commensurate (C') phase transition sequence with decreasing temperature [7]. In the N phase, which has an orthorhombic lattice with space group  $\text{Abma}$  ( $Z = 4$ ), the propylammonium ions are disordered between two equivalent orientations, related by a mirror plane perpendicular to the *b*-axis [11]. In the IC phase with the superspace group  $\text{P}_{s11}^{\text{Abma}}$ , the modulation vector  $\mathbf{q} = 0.418\mathbf{b}^*$  was reported to be independent of temperature [12]. The IC modulation of the  $\text{CdCl}_6$  octahedra is related to rotation around the *a*-axis and translation along the *c*-axis. Thus, the position of the nitrogen atoms in the propylammonium chains gets modulated through hydrogen bonds to halogens [12]. In the C phase with space group  $\text{Pbca}$  ( $Z = 4$ ), the angular fluctuation of octahedra about the *a*-axis is locked-in, and the orientation of the propylammonium ions is ordered [12].

In the present study, temperature dependences of the  $^1\text{H}$  NMR spin-lattice relaxation time  $T_1$  in PACC and in a partially deuterated analogue ( $n\text{-C}_3\text{H}_7\text{ND}_3)_2\text{CdCl}_4$  (PACC-*d*<sub>3</sub>),  $^2\text{H}$  NMR spectra in each phase of PACC-*d*<sub>3</sub>, and  $^{13}\text{C}$  MAS NMR spectra and  $T_1$  in PACC at room temperature were measured in order to clarify the cation dynamics.

## 2. Experimental

PACC crystals were obtained by slow cooling from about 350 K to room temperature of an aqueous solution containing stoichiometric amounts of cadmium chloride and propylammonium chloride with an additional small amount of hydrochloric acid. Chemical analysis, found: C = 19.26, H = 5.48, N = 7.38(%); calcd.: C = 19.24, H = 5.38, N = 7.48(%). PACC- $d_3$  was prepared by crystallizing PACC three times from heavy water. The obtained powdered crystals were put in glass tubes, dried *in vacuo* and then sealed with nitrogen gas for differential thermal analysis (DTA) and NMR measurements. In the DTA measurements the sample temperature was determined within  $\pm 0.2$  K with a chromel-constantan thermocouple.

The  $^1\text{H}$  NMR spin-lattice relaxation times  $T_1$  were measured with home made pulsed NMR spectrometers at a Larmor frequency of 41.6 MHz using the  $180^\circ\text{-}\tau\text{-}90^\circ$  pulse sequence in temperature ranges 92 - 360 K and 92 - 350 K for PACC and PACC- $d_3$ , respectively. The accuracy of the temperature measurement was  $\pm 0.2$  K and the uncertainty in  $^1\text{H}$   $T_1$  was estimated within 10%.  $^2\text{H}$  NMR spectra in PACC- $d_3$  were measured with a Bruker MSL-300 NMR system at 46.1 MHz in a temperature-range 131 - 356 K. The sample temperature was controlled within  $\pm 1$  K with a VT-1000 temperature controller and determined by a copper-constantan thermocouple with the same accuracy. A  $^{13}\text{C}$  MAS NMR spectrum in PACC at room temperature (ca. 295 K) was taken at 67.9 MHz using a JEOL EX-270 spectrometer. The sample was rotated at 4 kHz. The spectrum was obtained by Fourier transform of free induction decay accumulated under  $^1\text{H}$  decoupled condition. The inversion recovery method was used in the  $^{13}\text{C}$   $T_1$  measurements. For the standard of  $^{13}\text{C}$  NMR chemical shift, adamantane was used, in which the two kinds of carbons denote 29.5 and 38.6 ppm. The uncertainty in  $^{13}\text{C}$   $T_1$  was estimated to be within 20%.

## 3. Results and Discussion

### 3.1. Phase Transition Temperatures Observed by DTA

DTA thermograms measured on heating showed endothermic anomalies due to phase transitions at  $101.4 \pm 1$ ,  $155.4 \pm 0.5$ , and  $178.8 \pm 1$  K in PACC. They

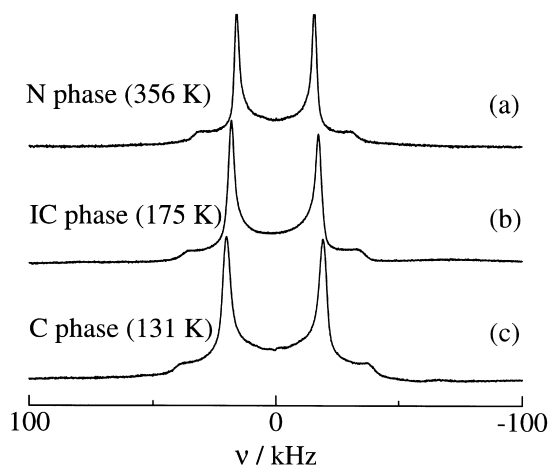


Fig. 1.  $^2\text{H}$  NMR spectra in PACC- $d_3$  observed at 356 K in N phase (a), at 175 K in IC phase (b), and at 131 K in C phase (c).

agree well with the reported phase transition temperatures  $T_C = 105.5$ ,  $T_C = 156.8$  and  $T_{IC} = 178.7$  K in PACC [10], respectively, and at  $101.2 \pm 1$ ,  $158.4 \pm 0.5$ , and  $178.0 \pm 1$  K in PACC- $d_3$ . The difference in  $T_C$  observed in PACC and PACC- $d_3$  suggests that the mechanism of the C-IC phase transition concerns the hydrogen-bond.

### 3.2. $^2\text{H}$ NMR Spectra in PACC- $d_3$

$^2\text{H}$  NMR spectra in PACC- $d_3$  showed line-shapes with an asymmetry parameter of the electric field gradient  $\eta \sim 0$  in the whole temperature range studied, as shown in Figure 1. From the X-ray structural analysis, a disorder of the cation has been expected in the N phase [11]. We have examined whether the NMR line-shape can be explained by assuming a 2-site jump of the cation in the N phase. Using the jumping angle of about  $21^\circ$  which was estimated from the reported structure [11],  $\eta = 0.05$  was evaluated for the motionally averaged EFG tensor of the deuterium [13]. With this value of  $\eta$  the line-shape is almost indistinguishable with  $\eta = 0$ , so that the 2-site jump does not conflict with the observed line-shape. The quadrupole coupling constant  $e^2Qqh^{-1}$  was calculated from the line-shape by assuming  $\eta = 0$  in the C phase, where the cation is expected in ordered state, and  $\eta = 0.05$  in the IC and N phases. The temperature dependence of  $e^2Qqh^{-1}$  is shown in Figure 2. The  $e^2Qqh^{-1}$  value of 52 kHz at 131 K in the C phase is already smaller than  $e^2Qqh^{-1}_{\text{ND}_3} = 57$  kHz calculated

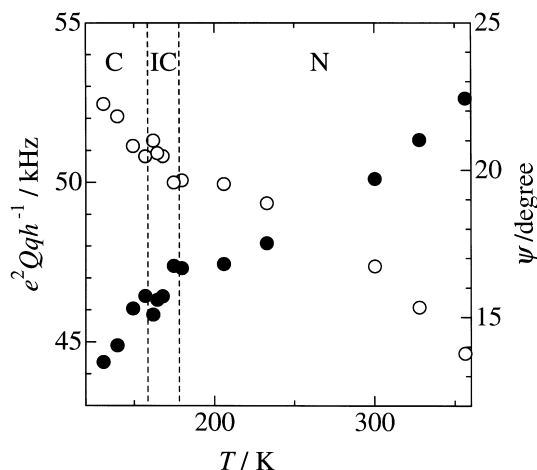


Fig. 2. Temperature dependence of the quadrupole coupling constant  $e^2Qqh^{-1}$  (○) determined from  $^2\text{H}$  NMR line-shapes observed in PACC- $d_3$  assuming  $\eta = 0$  in the C phase and  $\eta = 0.05$  (2-site jump with the angle  $2\theta = 21.25^\circ$ ) in the N and IC phases. The vertical lines show the transition temperatures observed by DTA. The angle  $\psi$  (●) which was calculated from (1) and (2) in the text is also shown.

for rotating  $\text{-ND}_3^+$  assuming a tetrahedral geometry and  $(e^2Qqh^{-1})_{\text{Rigid}} = 173$  kHz, which was reported for rigid  $\text{-ND}_3^+$  in ethylammonium chloride [14]. The value decreased gradually with increasing temperature, although the values are still larger than 38 kHz, the value which was calculated for the axial rotation of the cation as a whole about the principal axis of the moment of inertia assuming that the EFG principal axis of the rotating  $\text{-ND}_3^+$  makes  $27^\circ$  with it. This behaviour seems to be similar with the temperature dependence of the second moment of  $^1\text{H}$  NMR line reported by Blinc *et al.* [15]. This gradual decrease of  $e^2Qqh^{-1}$  is often observed in long chain compounds such as smectic liquid crystals and is explained by a random fluctuation of the molecular axis [16].

The  $e^2Qqh^{-1}$  value, reduced by the fluctuation, can be written as

$$e^2Qqh^{-1} = (e^2Qqh^{-1})_{\text{ND}_3} S \quad (1)$$

and

$$S = \frac{\langle 3 \cos^2 \phi - 1 \rangle}{2} = \frac{3 \cos^2 \psi - 1}{2}. \quad (2)$$

Here  $S$  is an order parameter which describes the degree of fluctuation [17],  $\phi$  is the angle between a principal axis of the EFG tensor and the fluctuation

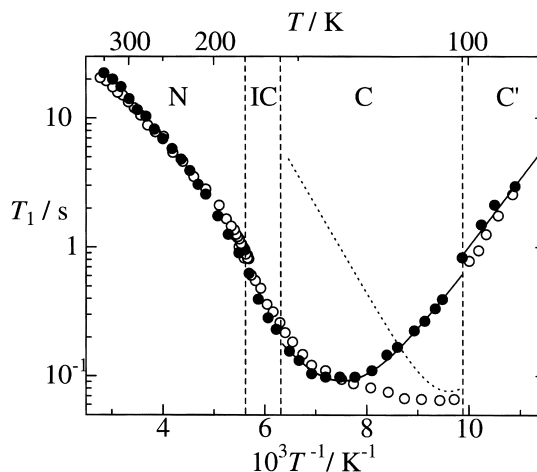


Fig. 3. Temperature dependences of the  $^1\text{H}$  NMR  $T_1$  observed at 41.6 MHz in PACC (○) and PACC- $d_3$  (●). The vertical lines show the transition temperatures observed by DTA for PACC- $d_3$ , and the solid lines in the C and C' phases are best-fitted curves for PACC- $d_3$ , applying (3) and (4) in the text. The broken line in the C phase indicates the contribution from the  $\text{NH}_3^+$  rotation in PACC.

axis of the molecule, and the brackets denote the statistical average. The angle  $\psi$  is defined as  $\cos \psi$  giving the root mean square of  $\cos \phi$ . The temperature dependence of  $\psi$  is also shown in Figure 2.

### 3.3. $^1\text{H}$ NMR $T_1$ Measurements

The recovery of  $^1\text{H}$  magnetization could be explained by a single  $T_1$  value in the whole temperature region including the IC phase. This result differs from the previous report by Blinc *et al.*, where the recovery was described by a sum of two exponential terms in the IC phase. In the case of the relaxation caused by the fluctuation of magnetic dipole-dipole interaction due to molecular motions, the relaxation rate  $T_1^{-1}$  can be represented by superposition of the BPP-type functions [18] for each motional mode,

$$T_1^{-1} = \sum C \left( \frac{\tau_c}{1 + \omega^2 \tau_c^2} + \frac{4\tau_c}{1 + 4\omega^2 \tau_c^2} \right) \quad (3)$$

where  $C$ ,  $\omega$ ,  $\tau_c$  denote the motional constant, the  $^1\text{H}$  Larmor frequency, and the correlation time of the motion, respectively. Assuming an Arrhenius-type relation,  $\tau_c$  is represented by the activation energy  $E_a$  of the motional process as follows,

$$\tau_c = \tau_0 \exp(E_a/RT). \quad (4)$$

Table 1. Motional constants  $C'$  and activation energies  $E_a$  derived by curve fitting of the temperature dependence of  $^1\text{H } T_1$  observed in PACC and PACC- $d_3$ .

	$C/10^9\text{s}^{-2}$	$E_a/\text{kJ mol}^{-1}$	Motional mode
PACC			
N phase ( $T > 280\text{ K}$ )	–	$8.0 \pm 1$	
C phase	2.0	$10 \pm 1$	$-\text{CH}_3$ rotation
	2.4	$13 \pm 1$	$-\text{NH}_3^+$ rotation
C' phase	–	$12 \pm 1$	$-\text{CH}_3$ rotation
PACC- $d_3$			
N phase ( $T > 280\text{ K}$ )	–	$8.5 \pm 1$	
C phase	2.0	$9.6 \pm 1$	$-\text{CH}_3$ rotation
C' phase	–	$10 \pm 1$	$-\text{CH}_3$ rotation

Here  $\tau_0$  denotes the correlation time at infinite temperature.

Temperature dependences of  $^1\text{H}$  NMR  $T_1$  on PACC and PACC- $d_3$  seem to be similar except for the low temperature region in the C phase, as shown in Figure 3. In the C phases of PACC- $d_3$  and PACC, the  $T_1$  curve can be reproduced by one and two BPP-curves, respectively. The BPP-curve of PACC, showing a minimum at higher temperature, is almost the same as that of PACC- $d_3$ . This implies that these curves are from the  $-\text{CH}_3$  rotation, and the other curve in PACC, showing a minimum at lower temperature, is from the  $-\text{NH}_3^+$  rotation. In the N phase, the temperature dependence of  $T_1$  becomes gentle gradually with increasing temperature, as shown in Figure 3. This may be explained by taking the 2-site jump and / or the molecular axis fluctuation into account. The best-fitted motional parameters in the C and C' phases of PACC and PACC- $d_3$ , and the activation energies in the high temperature region in the N phase of each compound are listed in Table 1.

#### 3.4. A $^{13}\text{C}$ MAS NMR Spectrum and $T_1$ Measurements

As shown in Fig. 4, the  $^{13}\text{C}$  MAS NMR spectrum observed in PACC gave three peaks at  $12.6 \pm 0.2$ ,  $21.5 \pm 0.2$ , and  $43.7 \pm 0.2$  ppm, which can be assigned to carbons in methyl, the middle methylene, and the end methylene groups, respectively.  $^{13}\text{C}$  NMR  $T_1$  values are  $7 \pm 1$ ,  $17 \pm 5$ , and  $20 \pm 6$  s for the 12.6, 21.5, and 43.7 ppm lines, respectively.  $^{13}\text{C } T_1$  is dominated

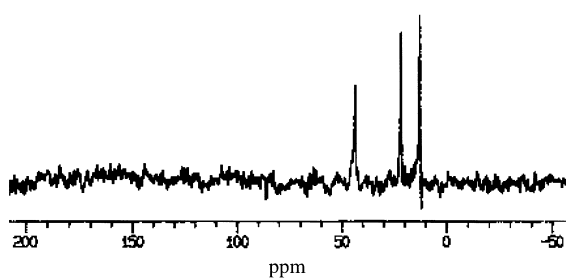


Fig. 4.  $^{13}\text{C}$  MAS NMR spectrum observed at room temperature in PACC.

usually by the fluctuation of the anisotropic chemical shift, and the  $T_1$  becomes short with larger amplitude of molecular motions [19]. This implies that the amplitude of the cationic motion is enhanced at the C-end, that is, the N-end of the organic cation is fixed on the inorganic layer through N-H...Cl hydrogen bonds.

#### 4. Conclusion

Phase transition temperatures in PACC- $d_3$  were determined by DTA. The difference in the C-IC phase transition temperature observed in PACC and PACC- $d_3$  suggests that the mechanism of the phase transition concerns a change of hydrogen-bond. The cationic motion as a whole, being associated with the fluctuation of the molecular axis is expected to be gradually excited with increasing temperature. The fact that the  $^{13}\text{C}$  MAS NMR  $T_1$  decreased with increasing distance from the  $-\text{NH}_3^+$  group implies that the amplitude of the cationic motion is enhanced at the counter side of the  $-\text{NH}_3^+$  group due to the N-H...Cl hydrogen bonds.

#### Acknowledgements

The authors are grateful to the Chemical Analysis Centre, University of Tsukuba, for elemental analysis. This work was partly supported by Grant-in-Aid for scientific research (B) No. 12440192 from the Ministry of Education, Science, Sports and Culture, by Nihon University Research Grant for Assistants, and by Grant from the Ministry of Education, Science, Sports and Culture to promote advanced scientific research.

- [1] C. Q. Qu, T. Kondo, H. Sakakura, K. Kumata, Y. Takahashi, and R. Ito, *Solid State Commun.* **79**, 245 (1991).
- [2] G. C. Papavassiliou, *Prog. Solid State Chem.* **25**, 125 (1997).
- [3] D. B. Mitzi, *Prog. Inorg. Chem.* **48**, 1 (1999).
- [4] R. Blinc, M. Kozelj, V. Rutar, I. Zupanicic, B. Žecš, H. Arend, R. Kind, and G. Chapuis, *Faraday Discuss. Chem. Soc.* **69**, 58 (1980).
- [5] R. Kind, *Ber. Bunsenges. Phys. Chem.* **87**, 248 (1983).
- [6] W. Depmeier, *Acta Crystallogr.* **B37**, 330 (1981).
- [7] R. Mokhlisse, M. Couzi, N. B. Chanh, Y. Haget, C. Hauw, and A. Meresse, *J. Phys. Chem. Solids* **46**, 187 (1985).
- [8] J. Etxebarria, I. Ruiz-Larrea, M. J. Tello, and A. López-Echarri, *J. Phys. C: Solid State Phys.* **21**, 1717 (1988).
- [9] Y. Abid, M. Kamoun, A. Daoud, F. Romain, and A. Lautie, *Phase Transitions* **40**, 239 (1992).
- [10] M. A. White, N. W. Granville, N. J. Davies, and L. A. K. Staveley, *J. Phys. Chem. Solids* **42**, 953 (1981).
- [11] G. Chapuis, *Acta Crystallogr.* **B34**, 1506 (1978).
- [12] B. Doudin and G. Chapuis, *Acta Crystallogr.* **B44**, 495 (1988).
- [13] R. Ikeda, A. Kubo, and C. A. McDowell, *J. Phys. Chem.* **93**, 7315 (1989).
- [14] M. J. Hunt and A. L. Mackay, *J. Magn. Reson.* **15**, 402 (1974).
- [15] R. Blinc, M. Burgar, B. Lozar, J. Seliger, J. Slak, and V. Rutar, *J. Chem. Phys.* **66**, 278 (1977).
- [16] J. W. Doane, in F. J. Owens et al. (eds), *Magnetic Resonance of Phase Transitions*, Academic Press, New York 1979.
- [17] A. Saupe and W. Maier, *Z. Naturforsch.* **16a**, 816 (1961).
- [18] A. Abragam, *The Principles of Nuclear Magnetism*, Oxford University Press, London 1961.
- [19] B. C. Gerstein and C. R. Dybowski, *Transient Techniques in NMR of Solids*, Academic Press Inc., London 1985.